

Article

Hydrochemical Characteristics and Risk Assessment of Tongzi River, Guizhou Province, Southwest China

Jiemei Lü ^{1,2} and Yanling An ^{1,2,*}

¹ The College of Resources and Environmental Engineering, Guizhou Institute of Technology, Guiyang 550003, China

² Key Laboratory of Karst Georesources and Environment, Ministry of Education, College of Resources and Environmental Engineering, Guizhou University, Guiyang 500025, China

* Correspondence: anyanling@git.edu.cn; Tel.: +86-150-8590-7470

Abstract: This study collected 31 water samples from the Tongzi River, Guizhou Province, Southwest China to conduct a risk assessment to understand the hydrochemical characteristics and major ion sources of irrigation and drinking water quality and their effects on human health. The results showed that ion abundance in the Tongzi River is Ca^{2+} (66%) > Mg^{2+} (24%) > $\text{K}^+ + \text{Na}^+$ (10%) for cations and HCO_3^- (75%) > SO_4^{2-} (21%) > Cl^- (4%) for anions. Additionally, the hydrochemical type of the water is Ca-Mg- HCO_3 , controlled by carbonate weathering. Methods including ion ratios, principal component analysis (PCA), and correlation analysis (CA) were used to analyze the source of main ions in the river water. PC1, with the most significant variance (54.9%), decides the hydrochemical characteristics and is affected by the positive loadings of SO_4^{2-} (0.92), pH (0.85), Ca^{2+} (0.80), Cl^- (0.72), Na^+ (0.66), NO_3^- (0.65), and K^+ (0.57). PC2 explains 19.2% of the total variance, with strong positive loadings of Na^+ (0.75), K^+ (0.63) and Cl^- (0.59). Mg^{2+} (0.84) and HCO_3^- (0.85) exhibits high loadings in PC3, explaining 9.3% of the variance. The results showed that intensive agricultural activities in the basin were the main source of nitrate NO_3^- , whereas SO_4^{2-} was mainly derived from mining activities. The lower concentrations of Na^+ , K^+ , and Cl^- were from coal combustion, domestic wastewater discharge, and agricultural fertilizer applications. The study area was mainly affected by carbonate rock weathering; natural processes (mainly the weathering of carbonate rocks) were still the main origin of Ca^{2+} , Mg^{2+} , and HCO_3^- . Moreover, the United States Salinity Laboratory (USSL) diagram and the Wilcox diagram showed that 100% of the samples fell in the C2S1 zones, and the water quality had good suitability for irrigation. The health risk assessment (HRA) results showed that $\text{HQ}_{\text{NO}_3^-}$ was much larger than $\text{HQ}_{\text{NH}_4^+}$ and indicated that nitrate pollution dominated non-health hazards. About 6.5% of the samples in the tributaries represented an unacceptable risk for infants and children, and the HQ value for infants and children was always higher than that for adults. Additionally, the non-carcinogenic health risk of riverine ions for infants and children in the Tongzi River was very noteworthy, especially in the tributaries.

Keywords: hydrochemical characteristics; major ion sources; agricultural activities; risk assessment



Citation: Lü, J.; An, Y.

Hydrochemical Characteristics and Risk Assessment of Tongzi River, Guizhou Province, Southwest China. *Water* **2023**, *15*, 802. <https://doi.org/10.3390/w15040802>

Academic Editor: Tammo Steenhuis

Received: 28 November 2022

Revised: 15 February 2023

Accepted: 16 February 2023

Published: 18 February 2023



Copyright: © 2023 by the authors. Licensee MDPI, Basel, Switzerland. This article is an open access article distributed under the terms and conditions of the Creative Commons Attribution (CC BY) license (<https://creativecommons.org/licenses/by/4.0/>).

1. Introduction

River pollution generally comes from natural sources (weathering, salt domes, waterways, etc.) and anthropogenic sources (such as industrial wastewater, irrigation wastewater, domestic sewage, etc.) [1]. With the development of the economy and society, human activities have exacerbated river pollution [2,3], endangering the safety of agricultural irrigation water and drinking water, further posing a threat to human health [4,5]. For example, a high concentration of Na^+ in water will replace Ca^{2+} and Mg^{2+} in soil, reducing the permeability of the soil and its ability to form stable polymers, which is not conducive to plant growth [6,7]. Applying inorganic fertilizers and animal manure in agricultural areas has increased the nitrate content in water resources. The long-term drinking of

this water can induce diseases, such as methemoglobinemia, blue baby syndrome, and cancer, which seriously threaten human health [8–10]. Therefore, polluted rivers have become an environmental and health hazard. It is necessary to accurately analyze the sources of pollutants in river water and evaluate the water quality [11], as this is of great significance for the management and protection of the river water environment. At present, current assessments of water pollution include irrigation water quality, a risk assessment, etc. Common methods include the USSL diagram, the Wilcox diagram, irrigation water quality [12–15], the water-quality index (WQI) [16,17], and the health risk assessment [18].

Hydrochemical characteristics of river water result from long-term interactions between water and environments [19]. By analyzing the hydrochemical characteristics of river water and the concentration of the main ions (Na^+ , K^+ , Mg^{2+} , Ca^{2+} , F^- , Cl^- , NO_3^- , SO_4^{2-} , and HCO_3^-), the main contribution sources and migration of ions can be identified [20,21], which help to determine the controlling factors of hydrochemical evolution and assist in tracking pollutants from natural and anthropogenic processes [22]. Methods such as main ion ratios, isotope fractionation [23], principal component analysis (PCA), correlation analysis (CA), hierarchical cluster analysis (HACA), and discriminant analysis (CDA) are widely used to identify the source of riverine ions [21,24–30], and multivariate statistical analyses of fluvial ions could better help in identification [31].

Typical carbonate landforms develop in the karst area of Southwest China, where relatively barren and thin soil is formed [32,33]. Due to the unique geological conditions and strong karstification, the river system is susceptible and fragile [34]; therefore, the hydrochemical characteristics of rivers are greatly affected by the geological background. In particular, rock weathering, gypsum dissolution, ion exchange, and other processes affect the composition of water chemical ions [35,36]. The Tongzi River is located in the largest tributary of the Chishui River (a tributary without a dam in the Yangtze River), which belongs to the typical karst basin in Southwest China. The agricultural activities in the basin are frequent, and the rivers provide residents with irrigation and drinking water along the coast. In recent years, human activities, including the watershed cultivation of slope farmland and deforestation, have led to soil erosion and nonpoint source pollution [37]. Therefore, this study systematically analyzes the fluvial ions of the Tongzi River in the typical karst area, aiming to achieve the following: (1) determine the ionic composition of the river water; (2) identify the source of the main ions in the river; and (3) explore the potential irrigation hazards and health risks of water quality.

2. Materials and Methods

2.1. Study Area

The Tongzi River is the longest tributary of the Chishui River, which is a tributary of the Yangtze River in Southwest China, and the basin area is 3348 square kilometers, spanning Tongzi, Zunyi, Renhuai, Xishui, and other counties (Figure 1). The mainstream has a total length of 122 km, and annual precipitation varies between 850 and 1200 mm, with a maximum rainfall of 1550 mm. Additionally, the annual precipitation is mainly concentrated between May and August, accounting for about 60% of the yearly rainfall; it is a typical rain-source mountain river. The urban construction in the Tongzi River basin accounts for a relatively small proportion of land. It is relatively concentrated in the county, and the Tianmen River Reservoir in the upper reaches is the primary drinking water source of the county. The middle and lower reaches flow through the mountainous karst area with steep slopes and high terrain, which consists mainly of cultivated land and forest land. The proportion of cultivated land in the basin reached 28%, which has a major impact on the ecological environment through soil erosion caused by slope farmland. There are many mining enterprises in the basin, mainly in Tongzi County and Xishui County, and some coal plant sites in the lower reaches of the mainstream are built along the river. As shown in Figure 1c, the exposed lithology in the Tongzi River basin is mainly carbonate rock, silicate rock, and migmatite, which are mainly carbonate rocks. Basin outcrop strata include

Sinian, Triassic, Quaternary, etc., with the upper reaches composed of Paleozoic Permian and Triassic strata, with a wide limestone distribution, as well as shale and coal measures.

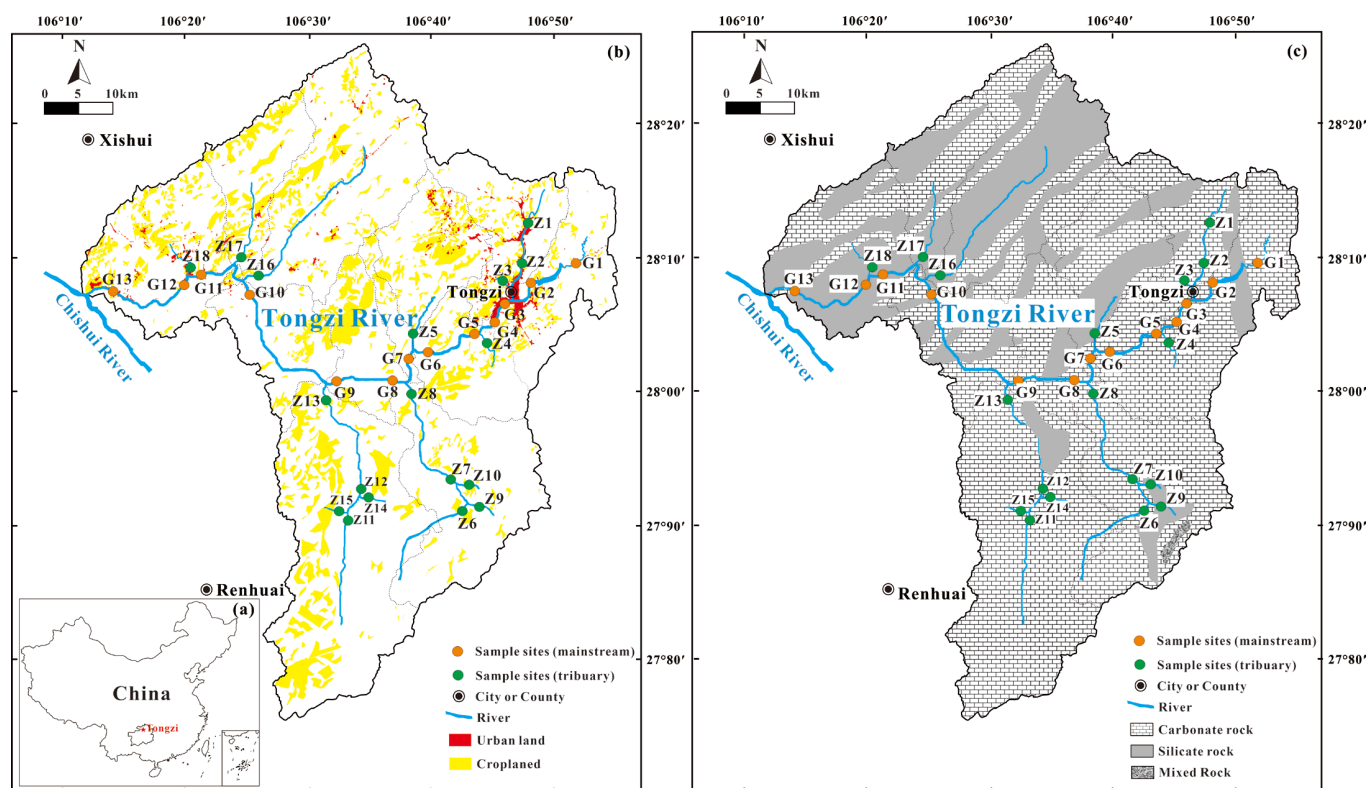


Figure 1. Location of Tongzi County in Southwest China (a), sampling maps of mainstream and tributaries of Tongzi River Basin under different land uses (b), the lithology distribution of Tongzi River watershed (c).

2.2. Sampling and Analysis

The implemented sampling campaign occurred during the basin's flood season in August of 2019, with a total of 31 samples obtained (13 samples (G1–G13) from the mainstream and 18 samples (Z1–Z18) from the tributaries) (Figure 1b). The sampling point information is shown in Figure 1. Water samples were collected at 0–20 cm below the surface using washed high-density polyethylene bottles. Temperature (T) and pH were measured in situ using WTW340i multiparameter water-quality meters (made in Germany, calibrated before sampling). On-site titration of HCO_3^- with 0.025 mol/L of HCl was carried out three times per water sample with an error of less than 5%. The collected river water samples were filtered on the same day (0.45 μm Millipore filter membrane), stored in a polyethylene bottle, and sealed in a refrigerator at 4 °C. Na^+ , K^+ , Ca^{2+} , Mg^{2+} , Cl^- , NO_3^- , F^- , and SO_4^{2-} were analyzed and determined via ion chromatography (ICS-1100, Thermo Fisher, Waltham, MA, USA, IonPac AG-19 anion exchange cartridge, and IonPac CS-12A cation exchange cartridge), and the test accuracy was better than $\pm 5\%$.

2.3. Assessment Method

2.3.1. Irrigation Water Quality

The Tongzi River is the most crucial water resource for agricultural irrigation in the basin, and its water quality directly affects the growth of surrounding crops. Sodium adsorption ratio (SAR) and soluble sodium percentage (Na%) are indicators that reflect the alkali (sodium) damage of the irrigation water. A more considerable SAR value indicates that the stronger the soil adsorption of sodium ions, the more difficult it is for the vegetation roots to absorb water [38]. The larger the Na% value, the worse the permeability of the soil,

thus affecting vegetation growth. For irrigation water quality, different irrigation water salinity and alkalinity levels affect soil quality attributes, thereby changing the farmland yield. To comprehensively evaluate the salinity and alkalinity hazards of irrigation water, the sodium adsorption rate and other indicators are commonly used. The soluble sodium percentage (Na%) and residual sodium carbonate (RSC) are calculated according to the ion equivalent concentration (meq/L) of river water [39].

$$\text{SAR} = \sqrt{2} \times \text{Na}^+ / \left(\text{Ca}^{2+} + \text{Mg}^{2+} \right)^{1/2} \quad (1)$$

$$\text{Na\%} = \text{Na}^+ / \left(\text{Ca}^{2+} + \text{Mg}^{2+} + \text{Na}^+ + \text{K}^+ \right) \times 100\% \quad (2)$$

$$\text{RSC} = (\text{HCO}_3^- - \text{CO}_3^{2-}) - (\text{Ca}^{2+} + \text{Mg}^{2+}) \quad (3)$$

2.3.2. Health Risk Assessment

The health risk assessment method is a quantitative analysis method for evaluating substances that are harmful to human health. Water pollutants come into contact with the human body mainly through drinking water and the skin, causing damage to human organs and threatening human health [40]. However, ingestion is identified as a more severe exposure pathway compared to the dermal route [41,42]. The average total nitrogen content in the Tongzi River basin was 2.85 mg/L [43], which is 1.4 times higher than the Chinese (GB3838-2002) V water-quality standard, and the main forms of nitrogen in natural rivers were NO_3^- and NH_4^+ . Therefore, according to the USEPA risk guidelines (USEPA 2004), the exposure doses of direct intake ($\text{ADD}_{\text{ingestion}}$) were calculated for NO_3^- and NH_4^+ as follows:

$$\text{ADD}_{\text{ingestion}} = C_w \times \text{IR} \times \text{EF} \times \text{ED} / (\text{BW} \times \text{AT}) \quad (4)$$

where $\text{ADD}_{\text{ingestion}}$ is the average daily exposure dose ($\text{mg} \cdot \text{kg}^{-1} \text{d}^{-1}$) from drinking water; C_w is the measured concentration of nitrate in water (mg/L); IR is the ingestion rate (L/day); EF is the exposure frequency (days/year); ED is the exposure duration (years); BW is the body weight (kg); and AT is the average time for non-carcinogens to stay in the body (days). Table 1 shows the parameters of the health risk assessment model for the assessment of the risk NO_3^- and NH_4^+ pose to human health.

Table 1. Parameters employed for human health risk assessment.

Parameters	Unit	Infants	Children	Adults	Reference
EF	$\text{d} \cdot \text{a}^{-1}$	365	365	365	[44]
IR	$\text{L} \cdot \text{d}^{-1}$	0.8	1.5	2	[45]
AT	d	$365 \times \text{ED}$	$365 \times \text{ED}$	$365 \times \text{ED}$	[46]
ED	a	1	12	30	[46]
BW	kg	10	20	70	[45]

The hazard quotient (HQ) is usually used to evaluate non-carcinogenic health risks, which was defined as:

$$\text{Hazard Quotient (HQ)} = \text{ADD}_{\text{ingestion}} / \text{RfD}_{\text{ingestion}} \quad (5)$$

where $\text{ADD}_{\text{ingestion}}$ is the average daily exposure dose ($\text{mg} \cdot \text{kg}^{-1} \text{d}^{-1}$), and $\text{RfD}_{\text{ingestion}}$ is the reference dose of different ions (1.6 and 0.97 ppm/day for NO_3^- and NH_4^+) [47]. When $\text{HQ} < 1$, the human health risk caused by pollutants is permissible, whereas when $\text{HQ} > 1$, non-carcinogenic effects should be considered.

2.4. Data Analysis

Principal component analysis (PCA) and a correlation matrix were carried out using SPSS 21.0 (IBM SPSS Statistics, Chicago, IL, USA) (PCA is a common method for exploring potential sources). A Piper diagram was created for the relationship between ion concentrations and physicochemical parameters in the Tongzi River, and Origin 2022 (OriginLab, Northampton, UK) was used to edit the graphs.

3. Results and Discussion

3.1. Hydrochemical Compositions of Tongzi River

The chemical characteristics of river water demonstrate its environmental properties and functions. The water temperature (T), dissolved oxygen (DO), pH value, electrical conductivity (EC), main ion concentrations, and the composition of river water all reflect the basic hydrochemical properties and characteristics of river water. The statistical results of the major ion concentrations and the water parameters (T, EC, pH, and DO) during the study period are listed in Table 2. The Tongzi River water temperature ranged from 20.0 to 29.0 °C with a mean value of 23.6 °C. The EC values ranged from 330 to 622 µS/cm with a mean value of 436 µS/cm, whereas the pH values varied between 8.54 and 9.36 with a mean value of 9.13, meaning the river waters were slightly alkaline. The CO_3^{2-} and CO_2 in the aqueous solution were negligible with regards to the carbonate equilibrium and the main inorganic carbon species in the Tongzi River was HCO_3^- . The total cationic charges ($\text{TZ}^+ = \text{Na}^+ + \text{K}^+ + 2\text{Mg}^{2+} + 2\text{Ca}^{2+}$) in the river water ranged from 3.33 to 6.37 meq·L⁻¹ (mean value of 4.55 meq·L⁻¹), and the total anionic charges ($\text{TZ}^- = \text{Cl}^- + \text{NO}_3^- + \text{HCO}_3^- + 2\text{SO}_4^{2-}$) in the river water ranged from 3.25 to 6.51 meq·L⁻¹ (mean value of 4.56 meq·L⁻¹). The mean value of the normalized inorganic charge balance ($\text{NICB} = (\text{TZ}^+ - \text{TZ}^-)/\text{TZ}^+$) [48,49] was generally <4% for each sampling campaign (Table S1), suggesting that the anions and cations in the Tongzi River were basically balanced.

Table 2. Values of Major Ions and Some Hydrogeochemical Parameters in the Tongzi River.

	Min	Max	Mean	SD	Chinese Guideline	WHO Guideline
T (°C)	20.0	29.0	23.6	2.9		
EC (µS/cm)	330	622	436	61		
pH	8.54	9.36	9.13	0.17	6.5–8.5	6.5–8.5
DO (mg/L)	1.24	13.01	8.91	2.37		
Na ⁺ (mmol/L)	0.06	0.58	0.20	0.11		
K ⁺ (mmol/L)	0.02	0.16	0.05	0.02		
Mg ²⁺ (mmol/L)	0.31	1.09	0.56	0.22		
Ca ²⁺ (mmol/L)	1.16	2.44	1.58	0.30		
F ⁻ (mmol/L)	0.004	0.011	0.007	0.002	0.05	0.08
Cl ⁻ (mmol/L)	0.03	0.51	0.14	0.10	7.05	7.05
NO ₃ ⁻ (mmol/L)	0.08	0.47	0.20	0.07	1.428	3.570
SO ₄ ²⁻ (mmol/L)	0.37	1.18	0.76	0.20	2.60	2.60
HCO ₃ ⁻ (mmol/L)	2.01	3.66	2.69	0.43		
NH ₄ ⁺ (mg/L)	0.01	2.65	0.25	0.46	0.036	0.107
SAR	0.06	0.49	0.20	0.09		
Na%	2.56	16.57	8.33	0.03		
RSC	0.16	1.26	0.53	0.26		

Note: the unit of corresponding values in the Chinese guidelines and WHO guidelines are converted to mmol/L.

As shown in Figure 2, the mean proportion of cations in the Tongzi River water followed a decreasing order of Ca^{2+} (66%) > Mg^{2+} (24%) > $\text{K}^+ + \text{Na}^+$ (10%), and the dominant anion was HCO_3^- which, on average, accounted for 75% of the total anions, followed by SO_4^{2-} (21%) and Cl^- (4%). These findings are basically consistent with the hydrochemical characteristics of the Chishui River [47], where the dominant cations were found to be Ca^{2+} and Mg^{2+} , whereas the dominant anions were HCO_3^- and SO_4^{2-} ; these data essentially comply with the component characteristics of major ions in the

Guizhou karst rivers, and the hydrochemical type of the Tongzi River water was Ca-Mg-HCO₃, controlled by carbonate weathering. Compared with the Changjiang River (urban area), the Jialing River (Chongqing area), and the Nanming River, the regions where carbonate rocks were distributed were all dominated by HCO₃[−] and Ca²⁺. The Tongzi River has a rich proportion of SO₄^{2−} (21%), which is obviously higher than in the Changjiang River [50,51] (16% and 10%), the Nanming River [31] (17%), and the Jialing River [26] (14%). Although the SO₄^{2−} content of the Tongzi River is higher than that of the above river, it is probably subjected to human activities and the dissolution of sulfide oxidation (e.g., pyrite) [47,52]. The Na⁺+K⁺ and Cl[−] contents are relatively low, and the proportions are obviously lower than in the Nanming River [31] (Na⁺+K⁺:26%, Cl[−]:10%) and the Jialing River [26] (Na⁺+K⁺:28%, Cl[−]:16%), and are much lower than in the Changjiang River [50,51] (Na⁺+K⁺:31% and 42%, Cl[−]: 13% and 24%), all of which are subject to the influence of different anthropogenic activities [26,31,47,50,51].

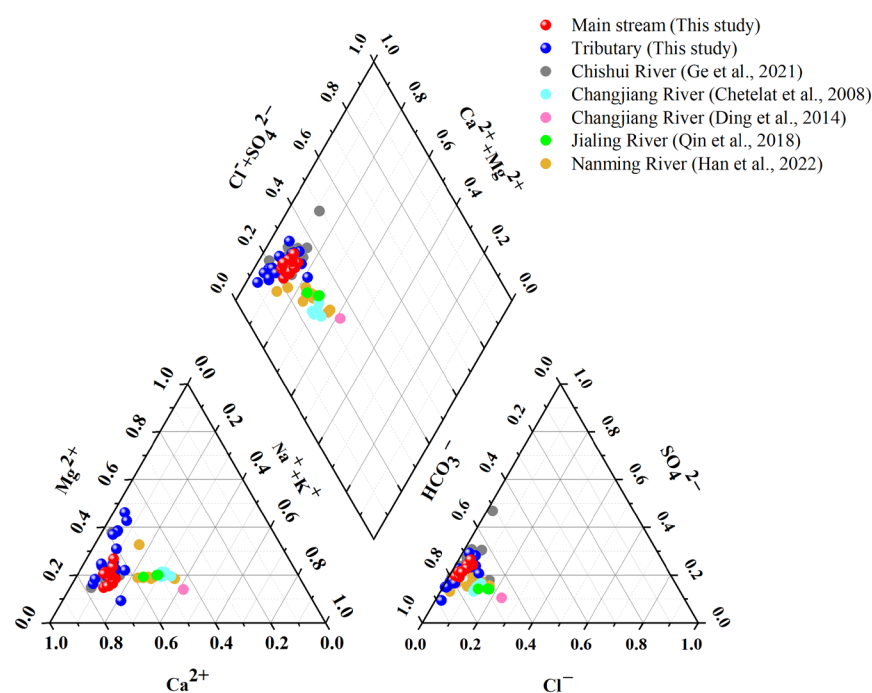


Figure 2. Piper diagrams representing the percentages of hydrochemical species in Tongzi River, Chishui River [47], Changjiang River [50,51], Jialing River [26], and Nanming River [31].

3.2. Sources of River Solutes

3.2.1. Correlation Matrix and PCA Analysis of Major Ions

Spearman's correlation among the major ionic components in the water allows for a systematic analysis of the interrelationships between the major ions. Based on their relationships, we can determine the source and identify the possible factors that affect the major ions [53]. Additionally, to further explore the source of the main ions in the Tongzi River basin, PCA was also used for analyses [54]. In general, KMO values below 0.5 are not desirable, whereas values from 0.5 to 0.7 are considered sufficient, and higher values (above 0.7) are outstanding [55]. The current study achieved a KMO value of 0.65; therefore, we used the correlation matrix and PCA to explore the source of major ions in the Tongzi River basin. For the Tongzi River, three principal components (PCs) with eigenvalues above 1 were retained, which explains 83.4% of the total variance (Table 3). PC1, with the most significant variance (54.9%), decides the hydrochemical characteristics and is affected by positive loadings of SO₄^{2−} (0.92), pH (0.85), Ca²⁺ (0.80), Cl[−] (0.72), Na⁺ (0.66), NO₃[−] (0.65), and K⁺ (0.57). PC2 explains 19.2% of the total variance, with strong positive loadings of Na⁺ (0.75), K⁺ (0.63) and Cl[−] (0.59). Mg²⁺ (0.84) and HCO₃[−] (0.85) exhibited high loadings in PC3, explaining 9.3% of the variance.

Table 3. Varimax-rotated component matrix for water ions in the Tongzi River.

Variable	PC1	PC2	PC3	Communalities
EC	−0.16	−0.87	−0.06	0.78
pH	0.85	0.35	0.38	0.98
Na ⁺	0.66	0.63	−0.19	0.87
K ⁺	0.57	0.75	−0.11	0.89
Mg ²⁺	0.03	−0.44	0.84	0.90
Ca ²⁺	0.80	0.47	0.03	0.86
Cl [−]	0.72	0.59	0.01	0.86
NO ₃ [−]	0.65	0.38	0.05	0.56
SO ₄ ^{2−}	0.92	0.04	−0.04	0.84
HCO ₃ [−]	0.28	0.23	0.85	0.86
F [−]	0.55	−0.04	−0.68	0.76
eigenvalues	6.04	2.11	1.03	
variance (%)	54.86	19.19	9.33	
cumulative (%)	54.86	74.05	83.38	

Note: extraction method—principal component analysis; rotation method—varimax with Kaiser normalization.

PC1 and PC2 exhibited high positive loadings (>0.50) of Na⁺, K⁺, and Cl[−], and there was a strong positive correlation among Na⁺, K⁺, and Cl[−]. There is no obvious evaporite (KCl and NaCl) exposed in the river basin; therefore, in addition to rock-weathering sources, Na⁺, K⁺, and Cl[−] in the river water also have other anthropogenic sources, such as industrial (coal combustion) [20,56] and domestic wastewater discharge [48] and agricultural fertilizer [24]. Moreover, there are some coal mines in the basin, many villages and towns along the basin, and a large proportion of agricultural land. Samples from the Tongzi River presented low concentrations of Cl[−], Na⁺, and K⁺, which means that Na⁺, K⁺, and Cl[−] are mainly from coal combustion, rainfall [57], domestic wastewater discharge (NaCl), and agricultural fertilizer (KCl).

The results presented in Figure 3 show that SO₄^{2−} and Mg²⁺, and especially HCO₃[−] and Ca²⁺, were the ions with a high concentration in the river water. SO₄^{2−} and Ca²⁺ had a significant correlation, but sulfate was also strongly correlated with other ions, such as Na⁺, K⁺, and Cl[−]; the significance of SO₄^{2−} and anthropogenic input ions (Na⁺, K⁺, and Cl[−]) is higher, inferring that they may be from the same source. SO₄^{2−} is derived from human activities and the dissolution of sulfide oxidation (e.g., pyrite) [47,52], which is consistent with the presence of SO₄^{2−} in the whole Chishui River [58]. HCO₃[−], Ca²⁺, and Mg²⁺ are significantly correlated, indicating that carbonate weathering inputs account for their high proportion. In addition, Mg²⁺, Ca²⁺, and HCO₃[−] mainly come from the dissolution of dolomite and limestone, which is consistent with the main rock types in the study area [31,59,60].

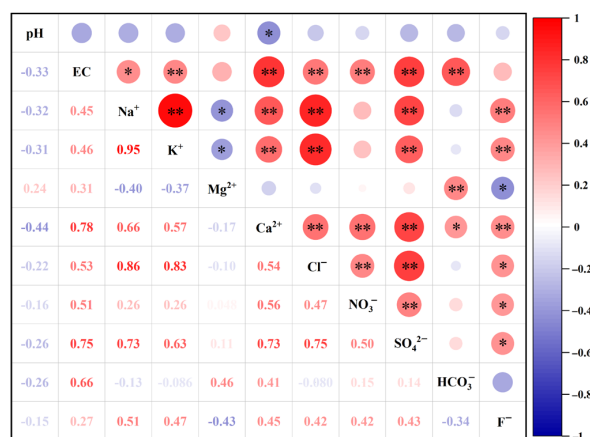


Figure 3. Spearman's correlation for the Tongzi River ions and other parameters; an asterisk (*) denotes $p < 0.05$; two asterisks (**) denote $p < 0.01$.

According to previous studies, nitrate mainly comes from anthropogenic sources, such as urban sewage, mobile emission sources (transportation) [61,62], industrial pollution [63], agricultural nitrogen fertilizers [64], and animal waste [65]. In this study, NO_3^- exhibited a much higher concentration (mean 12.7 mg/L) than that in the Xijiang River, where extensive agricultural activities exist (with a high average value of 6.4 mg/L) [65]. Furthermore, the high correlation between Cl^- and NO_3^- in PC1 indicates that their sources are consistent and are closely related to the use of agricultural nitrogen fertilizers [66]. Therefore, NO_3^- mainly comes from agricultural nitrogen fertilizers.

3.2.2. Mineral Dissolution

The Gibbs diagram [67] method defined three mechanisms (evaporation–crystallization, rock dominance, and atmospheric precipitation) that control world surface water chemistry. The relationship between TDS and $\text{Na}^+ / (\text{Na}^+ + \text{Ca}^{2+})$ and $\text{Cl}^- / (\text{Cl}^- + \text{HCO}_3^-)$ can be used to judge the main control types of the main ions in river water and the influencing factors of hydrochemical changes in the river basin [67]. As shown in Figure 4, the $\text{Na}^+ / (\text{Na}^+ + \text{Ca}^{2+})$ of most river samples in the Tongzi River is less than 0.6, and the $\text{Cl}^- / (\text{Cl}^- + \text{HCO}_3^-)$ is less than 0.2. All river sample points were from the rock-weathering control area and away from the atmospheric action zone, indicating that the ion composition of the river is mainly controlled by rock weathering, which is similar to that in the Yangtze River [26], the Xijiang River [68], the Wujiang River [69], and other large basins in China, as well as the Qingshui River [70], the Chishui River [47], and other karst regions.

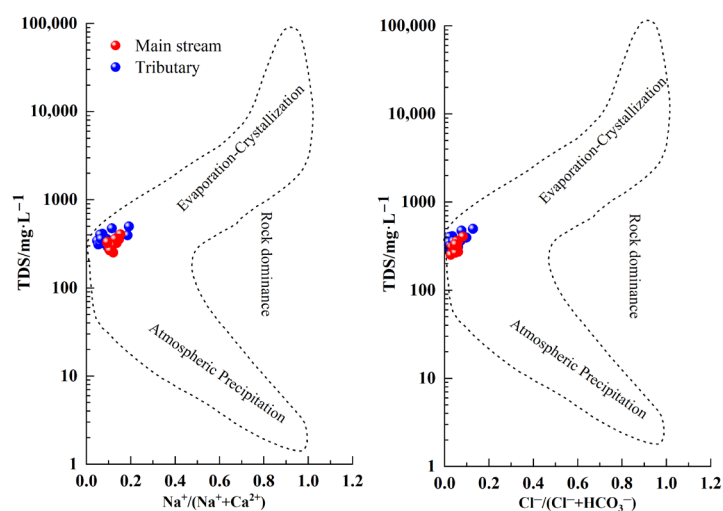


Figure 4. Gibbs plots of river water in the Tongzi River Basin [67].

For further analysis of rock-weathering types and to explore the source of the main ions generated by rock weathering in the region [71], end-member diagrams [72], including $\text{Mg}^{2+} / \text{Na}^+$ vs. $\text{Ca}^{2+} / \text{Na}^+$ (Figure 5a) and $\text{HCO}_3^- / \text{Na}^+$ vs. $\text{Ca}^{2+} / \text{Na}^+$ (Figure 5b), can be used to further determine the types of rock-weathering sources [58]. As shown in Figure 5a, the samples from the mainstream and tributaries of the Tongzi River basin were mainly concentrated in the vicinity of the carbonate rock end-member and between the carbonate rock and silicate rock end-member. Still, most of the points are biased toward the carbonate rock area. Some fall in the carbonate rock-weathering area, indicating that the study area is more affected by carbonate rock than silicate rock.

As shown in Figure 5c, most water samples fall to the right of the 1:1 line, which may be affected, to a certain degree, by silicate rock weathering or the cation exchange process [73,74]. The ratios of $\text{Ca}^{2+} + \text{Mg}^{2+}$ to HCO_3^- are used to characterize the dissolution of carbonate minerals' (such as calcite and dolomite) contribution to the chemical characteristics of river water [75]. Figure 5d shows that the water samples are mainly concentrated on the light side of the 1:1 line, indicating that the weathering of carbonate rocks is the main source of Ca^{2+} , Mg^{2+} , and HCO_3^- in the Tongzi River [76]. As shown in Figure 5e, all

the water samples are mainly concentrated on the 1:1 line, which indicates that the dissolution of carbonate and sulfate minerals dominate the hydrochemical characteristics of the Tongzhi River. In addition, the ratio between $\text{Na}^+ + \text{K}^+ - \text{Cl}^-$ and $\text{HCO}_3^- + \text{SO}_4^{2-} - \text{Ca}^{2+} - \text{Mg}^{2+}$ is commonly utilized to identify the influence of cation exchange [46,58,77]. The ratios of most water samples were near the 1:1 line, indicating that the cation exchange process significantly affects water hydrochemistry [7]. Figure 5f shows that all water samples fall on the left side of the 1:1 line, revealing that cation exchange does not affect the Tongzhi River.

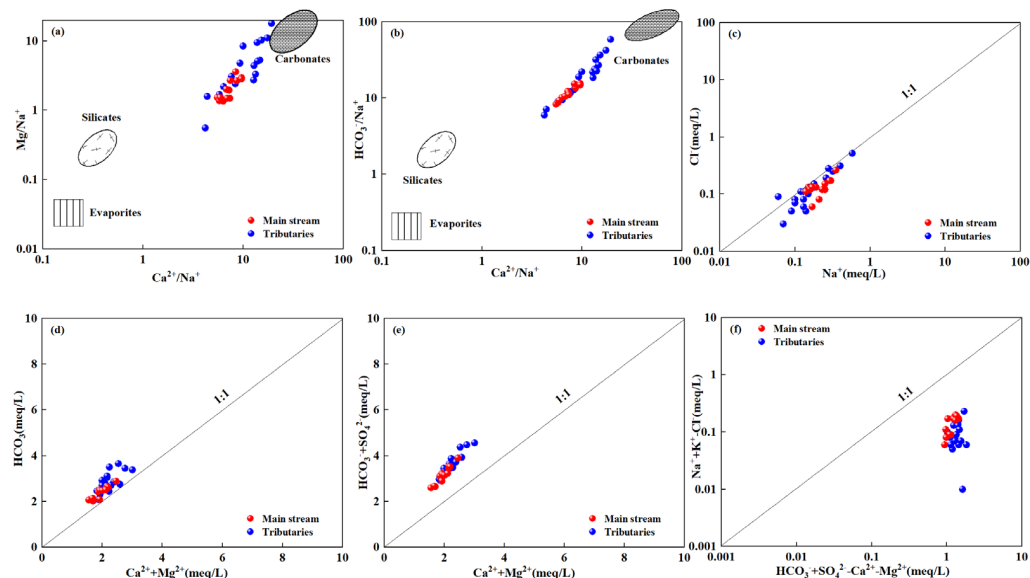


Figure 5. Plots of $\text{Ca}^{2+}/\text{Na}^+$ versus $\text{Mg}^{2+}/\text{Na}^+$ (a), $\text{Ca}^{2+}/\text{Na}^+$ versus $\text{HCO}_3^-/\text{Na}^+$ (b), Na^+ versus Cl^- (c), $(\text{Ca}^{2+} + \text{Mg}^{2+})$ versus HCO_3^- (d), $(\text{Ca}^{2+} + \text{Mg}^{2+})$ versus $(\text{HCO}_3^- + \text{SO}_4^{2-})$ (e), and $(\text{HCO}_3^- + \text{SO}_4^{2-} - \text{Ca}^{2+} - \text{Mg}^{2+})$ versus $(\text{Na}^+ + \text{K}^+ - \text{Cl}^-)$ (f) for the study area.

3.2.3. Anthropogenic Inputs

Human activities significantly impact the chemical characteristics of water bodies. In areas of intense human activities, anthropogenic inputs often influence rivers, with intensive human activities leading to elevated levels of Cl^- , NO_3^- , and SO_4^{2-} [78,79]. In addition, polluted water is generally considered to have high Cl^-/Na^+ , $\text{NO}_3^-/\text{Na}^+$, and $\text{SO}_4^{2-}/\text{Na}^+$ ratios [46,73]. Therefore, the present study used the Cl^-/Na^+ , $\text{NO}_3^-/\text{Na}^+$, and $\text{SO}_4^{2-}/\text{Na}^+$ ratios of the Tongzhi River in comparison with those from other rivers to further evaluate the ion ratio characteristics of rivers under different human influences (Figure 6a,b). The results show that the Tongzhi River has a higher ratio of $\text{NO}_3^-/\text{Na}^+$ than other urban rivers (Yangtze River, Jialing River, and Nanming River), and the water samples located close to agricultural activities are similar to those from the Chishui River, indicating that agricultural activity is an important source of NO_3^- in the Tongzhi River. In addition, Figure 6b shows that the Tongzhi River was also affected by industrial activities to a certain extent and is similar to the Chishui River, indicating that SO_4^{2-} is mainly derived from industrial activities.

3.3. Irrigation and Guideline-Based Water Quality

The Tongzhi River is a typical plateau agricultural river. The proportion of cultivated land in the basin is 18%. The crops are mainly wheat, corn, and rice; therefore, Tongzhi River water is an important water source for agricultural irrigation. Additionally, the irrigation water quality is almost equally important in ensuring food security and social and economic development [80]. The concentrations of inorganic ions in the Tongzhi River are also in line with the range given by the Chinese guidelines and the WHO guidelines. The suitable pH value of drinking water is suggested to be between 6.5 and 8.5. Still, most

water samples have unsuitable pH values because carbonate weathering causes karst rivers to have high pH [81].

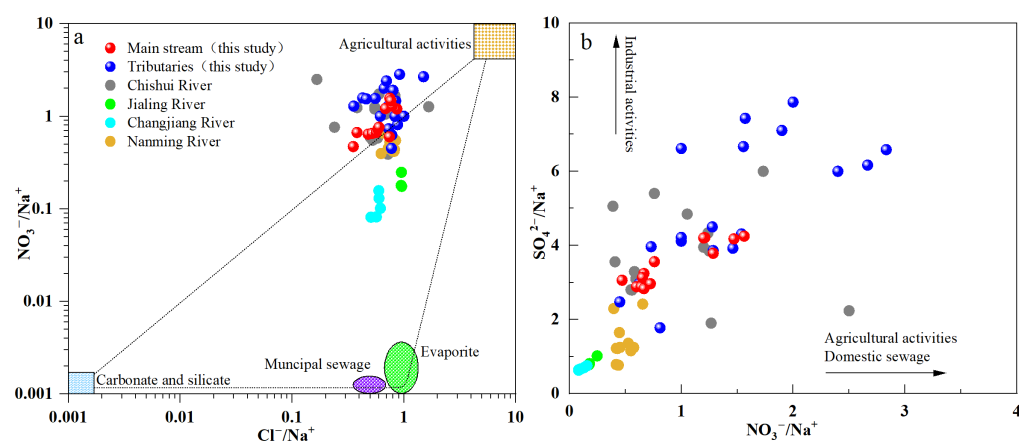


Figure 6. Plots of Cl^-/Na^+ versus $\text{NO}_3^-/\text{Na}^+$ (a) and $\text{NO}_3^-/\text{Na}^+$ versus $\text{SO}_4^{2-}/\text{Na}^+$ (b) for water samples of the Tongzi River, Chishui River [47], Changjiang River [50], Jialing River [26], and Nanming River [31].

The Na% ranged from 2.56 to 16.57%, with an average value of 8.21%, and the SAR varied from 0.06 to 0.49, with a mean value of 0.19. The United States Salinity Laboratory plot (Figure 7a) shows that 100% of the samples fell in the C2S1 zones, indicating a medium salinity hazard. In addition, according to the Wilcox diagram (Figure 7b), most samples were in the excellent to good section. In general, low sodium and moderate salinity hazards may exist in the Tongzi River, indicating a relatively suitable quality for irrigation without much harm to soil aggregates. In addition, the RSC value of the Tongzi River water sample exceeded 1.26 (Table S1), indicating the suitability of irrigation water.

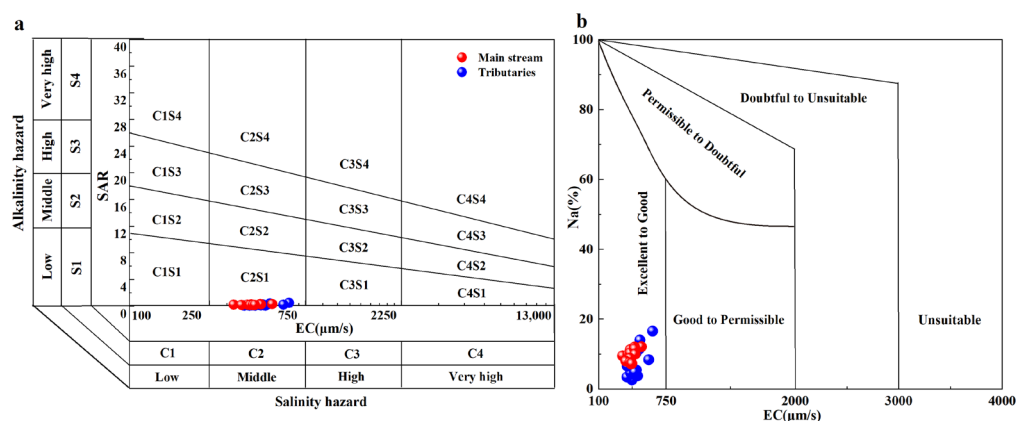


Figure 7. Salinity and alkalinity evaluation of irrigation water quality: (a) United States Salinity Laboratory (USSL) diagram and (b) Wilcox diagram.

3.4. Health Risk Assessment

A health risk assessment is a method used to assess possible harmful health effects in different groups of people [82]. The human body mainly absorbs toxic substances in the water body by drinking the water. The Tongzi River basin provides drinking water for nearby residents, especially those in the upstream Tianmen River Reservoir, as it is the main drinking water source in Tongzi County. NH_4^+ and NO_3^- in the water enter the human body mainly through the drinking of the water. Long-term consumption of water polluted by NH_4^+ and NO_3^- can lead to various diseases, such as leukemia, digestive system cancer, and blue baby syndrome [83]. Therefore, the present study used the model

recommended by the US Environmental Protection Agency to evaluate the potential risks to human health posed by the non-point source pollution (NSP).

The non-carcinogenic health risks of the total HQ value ($HQ_T = HQ_{NO_3^-} + HQ_{NH_4^+}$) in the Tongzi River were calculated (Figure 8c). The results of the HRA showed that the $HQ_{NO_3^-}$ values for infants, children, and adults were 0.25–1.46, 0.23–1.37, and 0.09–0.52, with mean values of 0.63, 0.59, and 0.23 (Figure 8a), respectively. The $HQ_{NH_4^+}$ values for infants, children, and adults were 0.001–0.219, 0.001–0.205, and 0–0.078, with mean values of 0.02, 0.019, and 0.007 (Figure 8b), respectively. This suggests that $HQ_{NO_3^-}$ is much larger than $HQ_{NH_4^+}$ and indicates that non-health hazards are dominated by nitrate pollution. For infants, children, and adults, the HQ_T of each ion and total HQ were higher than the hazard level (>1), indicating a higher health risk of the assessed ions. About 6.5% of the samples (Z3 and Z15) in the tributaries had an unacceptable risk for infants and children, and the HQ value for infants and children was always higher than that for adults, implying they face an increased risk from the riverine ions compared to adults. The non-carcinogenic health risk of riverine ions to infants and children in the Tongzi River is very noteworthy, especially in the tributaries.

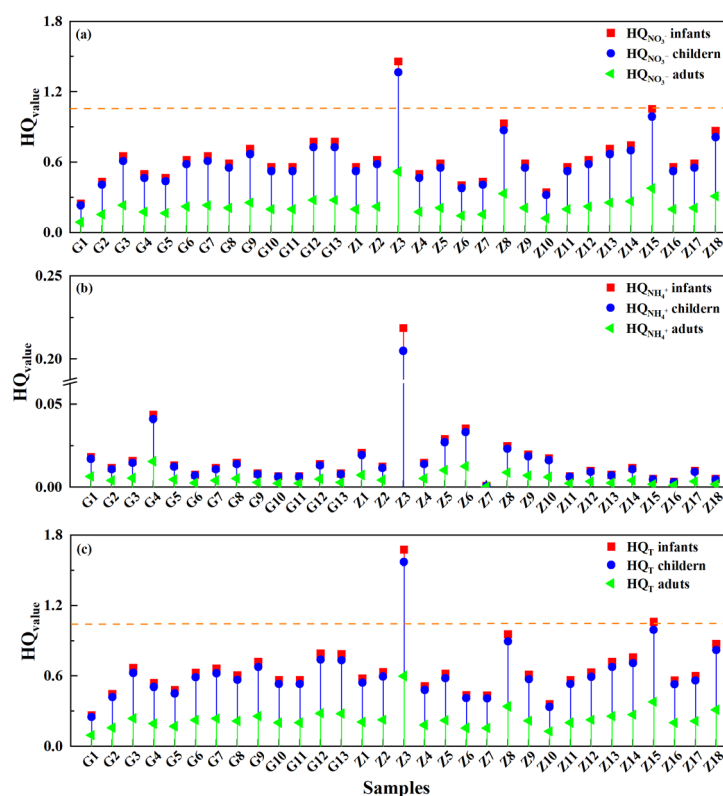


Figure 8. Non-carcinogenic health risk assessment in Tongzi River water. (a) HQ values of nitrate, (b) HQ values of ammonia, (c) total HQ value.

4. Conclusions

The present study collected 31 water samples from the Tongzi River to evaluate the hydrochemical characteristics, sources of river solutes, irrigation and guideline-based water quality, and risk to human health. The main conclusions of the present study are as follows: The ion abundance in the Tongzi River is Ca^{2+} (66%) $>$ Mg^{2+} (24%) $>$ $K^+ + Na^+$ (10%) for cations and HCO_3^- (75%) $>$ SO_4^{2-} (21%) $>$ Cl^- (4%) for anions. Additionally, the hydrochemical type of the water is Ca-Mg- HCO_3 , which is mainly controlled by carbonate weathering; thus, the weathering of carbonate rock is still the main origin of Ca^{2+} , Mg^{2+} , and HCO_3^- . In a typical agricultural river, compared to urban river sources, intensive agricultural activities in the basin are the main source of nitrate NO_3^- , whereas SO_4^{2-} mainly derives from industrial activities (coal mine). The irrigation and guideline-based

water-quality results showed that the concentrations of inorganic ions in the Tongzi River are also in line with the range given by the Chinese guidelines and the WHO guidelines, and that the irrigation water has good suitability. Moreover, the health risk assessment results showed that the amount of $HQ_{NO_3^-}$ is much larger than $HQ_{NH_4^+}$, and about 6.5% of the samples in the tributaries presented an unacceptable risk for infants and children, indicating that nitrate pollution dominates non-health hazards. Therefore, in the subsequent management of the water environment in the basin, the control of agricultural nonpoint source pollution should be strengthened to ensure the safety of water use in the basin.

Supplementary Materials: The following supporting information can be downloaded at: <https://www.mdpi.com/article/10.3390/w15040802/s1>, Table S1: The water parameters, major ion compositions, SAR, Na%, RSC, NICB of Tongzi River.

Author Contributions: J.L. methodology, formal analysis, investigation, data curation, and writing—original draft preparation. Y.A. writing—review and editing and funding acquisition. All authors have read and agreed to the published version of the manuscript.

Funding: This research was funded by the High-Level Talent Introduction Program for the Guizhou Institute of Technology (2019 [45]). The funder had no role in study design, data collection and analysis, decision to publish, or preparation of the manuscript.

Institutional Review Board Statement: Not applicable.

Informed Consent Statement: Not applicable.

Data Availability Statement: Not applicable.

Conflicts of Interest: The authors declare no conflict of interest.

References

- Gnanachandrasamy, G.; Dushiyanthan, C.; Jeyavel Rajakumar, T.; Zhou, Y. Assessment of hydrogeochemical characteristics of groundwater in the lower Vellar river basin: Using Geographical Information System (GIS) and Water Quality Index (WQI). *Environ. Dev. Sustain.* **2020**, *22*, 759–789. [CrossRef]
- Wang, J.; Jiang, Y.; Sun, J.; She, J.; Yin, M.; Fang, F.; Xiao, T.; Song, G.; Liu, J. Geochemical transfer of cadmium in river sediments near a lead-zinc smelter. *Ecotoxicological Environ. Saf.* **2020**, *196*, 110529. [CrossRef] [PubMed]
- Zeng, J.; Han, G.; Zhang, S.; Liang, B.; Qu, R.; Liu, M.; Liu, J. Potentially toxic elements in cascade dams-influenced river originated from Tibetan Plateau. *Environ. Res.* **2022**, *208*, 112716. [CrossRef] [PubMed]
- Liu, M.; Han, G.; Zhang, Q. Effects of agricultural abandonment on soil aggregation, soil organic carbon storage and stabilization: Results from observation in a small karst catchment, Southwest China. *Agric. Ecosyst. Environ.* **2020**, *288*, 106719. [CrossRef]
- Chen, L.; Liu, J.-r.; Hu, W.-f.; Gao, J.; Yang, J.-y. Vanadium in soil-plant system: Source, fate, toxicity, and bioremediation. *J. Hazard. Mater.* **2021**, *405*, 124200. [CrossRef]
- Yang, K.; Han, G.; Song, C.; Zhang, P. Stable H-O Isotopic Composition and Water Quality Assessment of Surface Water and Groundwater: A Case Study in the Dabie Mountains, Central China. *Int. J. Environ. Res. Public Health* **2019**, *16*, 4076. [CrossRef]
- Lu, T.; Li, R.; Ferrer, A.S.N.; Xiong, S.; Zou, P.; Peng, H. Hydrochemical characteristics and quality assessment of shallow groundwater in Yangtze River Delta of eastern China. *Environ. Sci. Pollut. Res.* **2022**, *29*, 57215–57231. [CrossRef]
- Ward, M.H.; Jones, R.R.; Brender, J.D.; De Kok, T.M.; Weyer, P.J.; Nolan, B.T.; Villanueva, C.M.; Van Breda, S.G. Drinking Water Nitrate and Human Health: An Updated Review. *Int. J. Environ. Res. Public Health* **2018**, *15*, 1557. [CrossRef]
- Schullehner, J.; Hansen, B.; Thygesen, M.; Pedersen, C.B.; Sigsgaard, T. Nitrate in drinking water and colorectal cancer risk: A nationwide population-based cohort study. *Int. J. Cancer* **2018**, *143*, 73–79. [CrossRef]
- Pennino, M.J.; Leibowitz, S.G.; Compton, J.E.; Hill, R.A.; Sabo, R.D. Patterns and predictions of drinking water nitrate violations across the conterminous United States. *Sci. Total Environ.* **2020**, *722*, 137661. [CrossRef]
- Tsering, T.; Abdel Wahed, M.S.M.; Iftekhar, S.; Sillanpää, M. Major ion chemistry of the Teesta River in Sikkim Himalaya, India: Chemical weathering and assessment of water quality. *J. Hydrol. Reg. Stud.* **2019**, *24*, 100612. [CrossRef]
- Zhang, B.; Song, X.; Zhang, Y.; Han, D.; Tang, C.; Yu, Y.; Ma, Y. Hydrochemical characteristics and water quality assessment of surface water and groundwater in Songnen plain, Northeast China. *Water Res.* **2012**, *46*, 2737–2748. [CrossRef] [PubMed]
- Xia, C.; Liu, G.; Xia, H.; Jiang, F.; Meng, Y. Influence of saline intrusion on the wetland ecosystem revealed by isotopic and hydrochemical indicators in the Yellow River Delta, China. *Ecol. Indic.* **2021**, *133*, 108422. [CrossRef]
- Zhou, Y.; Li, P.; Xue, L.; Dong, Z.; Li, D. Solute geochemistry and groundwater quality for drinking and irrigation purposes: A case study in Xinle City, North China. *Geochemistry* **2020**, *80*, 125609. [CrossRef]
- Elumalai, V.; Nethononda, V.G.; Manivannan, V.; Rajmohan, N.; Li, P.; Elango, L. Groundwater quality assessment and application of multivariate statistical analysis in Luvuvhu catchment, Limpopo, South Africa. *J. Afr. Earth Sci.* **2020**, *171*, 103967. [CrossRef]

16. Wong, Y.J.; Shimizu, Y.; He, K.; Nik Sulaiman, N.M. Comparison among different ASEAN water quality indices for the assessment of the spatial variation of surface water quality in the Selangor river basin, Malaysia. *Environ. Monit. Assess.* **2020**, *192*, 644. [\[CrossRef\]](#)
17. Wong, Y.J.; Shimizu, Y.; Kamiya, A.; Maneechot, L.; Bharambe, K.P.; Fong, C.S.; Nik Sulaiman, N.M. Application of artificial intelligence methods for monsoonal river classification in Selangor river basin, Malaysia. *Environ. Monit. Assess.* **2021**, *193*, 438. [\[CrossRef\]](#)
18. Gao, Z.; Han, C.; Xu, Y.; Zhao, Z.; Luo, Z.; Liu, J. Assessment of the water quality of groundwater in Bohai Rim and the controlling factors—A case study of northern Shandong Peninsula, north China. *Environ. Pollut.* **2021**, *285*, 117482. [\[CrossRef\]](#)
19. Xia, C.; Liu, G.; Meng, Y.; Jiang, F. Reveal the threat of water quality risks in Yellow River Delta based on evidences from isotopic and hydrochemical analyses. *Mar. Pollut. Bull.* **2022**, *177*, 113532. [\[CrossRef\]](#)
20. Xu, Z.; Liu, C.-Q. Chemical weathering in the upper reaches of Xijiang River draining the Yunnan–Guizhou Plateau, Southwest China. *Chem. Geol.* **2007**, *239*, 83–95. [\[CrossRef\]](#)
21. Li, X.; Han, G.; Liu, M.; Liu, J.; Zhang, Q.; Qu, R. Potassium and its isotope behaviour during chemical weathering in a tropical catchment affected by evaporite dissolution. *Geochim. Et Cosmochim. Acta* **2022**, *316*, 105–121. [\[CrossRef\]](#)
22. Wei, M.; Duan, P.; Gao, P.; Guo, S.; Hu, Y.; Yao, L.; Li, M. Exploration and application of hydrochemical characteristics method for quantification of pollution sources in the Danjiangkou Reservoir area. *J. Hydrol.* **2020**, *590*, 125291. [\[CrossRef\]](#)
23. Apollaro, C.; Tripodi, V.; Vespasiano, G.; De Rosa, R.; Dotsika, E.; Fuoco, I.; Critelli, S.; Muto, F. Chemical, isotopic and geotectonic relations of the warm and cold waters of the Galatro and Antonimina thermal areas, southern Calabria, Italy. *Mar. Pet. Geol.* **2019**, *109*, 469–483. [\[CrossRef\]](#)
24. Zhang, S.; Han, G.; Zeng, J.; Malem, F. Source tracing and chemical weathering implications of strontium in agricultural basin in Thailand during flood season: A combined hydrochemical approach and strontium isotope. *Environ. Res.* **2022**, *212*, 113330. [\[CrossRef\]](#) [\[PubMed\]](#)
25. Han, G.; Liu, C.-Q. Strontium isotope and major ion chemistry of the rainwaters from Guiyang, Guizhou Province, China. *Sci. Total Environ.* **2006**, *364*, 165–174. [\[CrossRef\]](#) [\[PubMed\]](#)
26. Qin, T.; Yang, P.; Groves, C.; Chen, F.; Xie, G.; Zhan, Z. Natural and anthropogenic factors affecting geochemistry of the Jialing and Yangtze Rivers in urban Chongqing, SW China. *Appl. Geochem.* **2018**, *98*, 448–458. [\[CrossRef\]](#)
27. Ghaemi, Z.; Noshadi, M. Surface water quality analysis using multivariate statistical techniques: A case study of Fars Province rivers, Iran. *Environ. Monit. Assess.* **2022**, *194*, 178. [\[CrossRef\]](#) [\[PubMed\]](#)
28. Wang, J.; Liu, G.; Liu, H.; Lam, P.K.S. Multivariate statistical evaluation of dissolved trace elements and a water quality assessment in the middle reaches of Huaihe River, Anhui, China. *Sci. Total Environ.* **2017**, *583*, 421–431. [\[CrossRef\]](#) [\[PubMed\]](#)
29. Zhan, S.; Wu, J.; Wang, J.; Jing, M. Distribution characteristics, sources identification and risk assessment of n-alkanes and heavy metals in surface sediments, Tajikistan, Central Asia. *Sci. Total Environ.* **2020**, *709*, 136278. [\[CrossRef\]](#)
30. Zhou, J.; Wu, Q.; Gao, S.; Zhang, X.; Wang, Z.; Wu, P.; Zeng, J. Coupled controls of the infiltration of rivers, urban activities and carbonate on trace elements in a karst groundwater system from Guiyang, Southwest China. *Ecotoxicol. Environ. Saf.* **2023**, *249*, 114424. [\[CrossRef\]](#)
31. Han, R.; Xu, Z. Riverine Hydrochemical Characteristics of a Typical Karst Urban Watershed: Major Ion Compositions, Sources, Assessment, and Historical Evolution. *ACS Earth Space Chem.* **2022**, *6*, 1495–1505. [\[CrossRef\]](#)
32. Zeng, J.; Yue, F.-J.; Wang, Z.-J.; Wu, Q.; Qin, C.-Q.; Li, S.-L. Quantifying depression trapping effect on rainwater chemical composition during the rainy season in karst agricultural area, southwestern China. *Atmos. Environ.* **2019**, *218*, 116998. [\[CrossRef\]](#)
33. Han, G.; Tang, Y.; Liu, M.; Van Zwieten, L.; Yang, X.; Yu, C.; Wang, H.; Song, Z. Carbon-nitrogen isotope coupling of soil organic matter in a karst region under land use change, Southwest China. *Agric. Ecosyst. Environ.* **2020**, *301*, 107027. [\[CrossRef\]](#)
34. Yue, F.-J.; Waldron, S.; Li, S.-L.; Wang, Z.-J.; Zeng, J.; Xu, S.; Zhang, Z.-C.; Oliver, D.M. Land use interacts with changes in catchment hydrology to generate chronic nitrate pollution in karst waters and strong seasonality in excess nitrate export. *Sci. Total Environ.* **2019**, *696*, 134062. [\[CrossRef\]](#)
35. Karunanidhi, D.; Subramani, T.; Roy, P.D.; Li, H. Impact of groundwater contamination on human health. *Environ. Geochem. Health* **2021**, *43*, 643–647. [\[CrossRef\]](#) [\[PubMed\]](#)
36. Fuoco, I.; Marini, L.; De Rosa, R.; Figoli, A.; Gabriele, B.; Apollaro, C. Use of reaction path modelling to investigate the evolution of water chemistry in shallow to deep crystalline aquifers with a special focus on fluoride. *Sci. Total Environ.* **2022**, *830*, 154566. [\[CrossRef\]](#) [\[PubMed\]](#)
37. Tian, Y.; Wang, S.; Bai, X.; Zhang, q.; Tao, j.; Zhang, Y.; Liang, M.; Zhou, G.; Lao, Y. Response og runoff of climate and human activities in Tongzi River Basin. *Res. Soil Water Conserv.* **2020**, *27*, 76–82.
38. Singh, V.; Singh, U. Assessment of groundwater quality of parts of Gwalior (India) for agricultural purposes. *Indian J. Sci. Technol.* **2008**, *1*, 1–5. [\[CrossRef\]](#)
39. Santacruz de León, G.; Ramos Leal, J.A.; Moran Ramírez, J.; López Álvarez, B.; Santacruz de León, E.E. Quality indices of groundwater for agricultural use in the Soconusco, Chiapas, Mexico. *Earth Sci. Res. J.* **2017**, *21*, 117–127. [\[CrossRef\]](#)
40. Xia, F.; Niu, X.; Qu, L.; Dahlgren, R.A.; Zhang, M. Integrated source-risk and uncertainty assessment for metals contamination in sediments of an urban river system in eastern China. *Catena* **2021**, *203*, 105277. [\[CrossRef\]](#)
41. Adimalla, N.; Li, P. Occurrence, health risks, and geochemical mechanisms of fluoride and nitrate in groundwater of the rock-dominant semi-arid region, Telangana State, India. *Hum. Ecol. Risk Assess. Int. J.* **2019**, *25*, 81–103. [\[CrossRef\]](#)

42. Adimalla, N.; Qian, H.; Nandan, M.J. Groundwater chemistry integrating the pollution index of groundwater and evaluation of potential human health risk: A case study from hard rock terrain of south India. *Ecotoxicol. Environ. Saf.* **2020**, *206*, 111217. [[CrossRef](#)] [[PubMed](#)]
43. Zhou, X.; An, Y.; Wu, Q.; Lv, J.; Gao, S.; Li, F. Response of Spatial Distribution of Nitrogen and Phosphorus to Human Activities in Mountainous Rivers—A Case Study of Tongzi River, a first-grade Tributary fo Chishui River. *Res. Soil Water Conserv.* **2021**, *28*, 179–185.
44. Chen, J.; Wu, H.; Qian, H. Groundwater Nitrate Contamination and Associated Health Risk for the Rural Communities in an Agricultural Area of Ningxia, Northwest China. *Expo. Health* **2016**, *8*, 349–359. [[CrossRef](#)]
45. Qasemi, M.; Afsharnia, M.; Zarei, A.; Farhang, M.; Allahdadi, M. Non-carcinogenic risk assessment to human health due to intake of fluoride in the groundwater in rural areas of Gonabad and Bajestan, Iran: A case study. *Hum. Ecol. Risk Assess. Int. J.* **2019**, *25*, 1222–1233. [[CrossRef](#)]
46. Liu, J.; Peng, Y.; Li, C.; Gao, Z.; Chen, S. Characterization of the hydrochemistry of water resources of the Weibei Plain, Northern China, as well as an assessment of the risk of high groundwater nitrate levels to human health. *Environ. Pollut.* **2021**, *268*, 115947. [[CrossRef](#)] [[PubMed](#)]
47. Ge, X.; Wu, Q.; Wang, Z.; Gao, S.; Wang, T. Sulfur isotope and stoichiometry-based source identification of major ions and risk assessment in Chishui River Basin, Southwest China. *Water* **2021**, *13*, 1231. [[CrossRef](#)]
48. Das, A.; Krishnaswami, S.; Sarin, M.; Pande, K. Chemical weathering in the Krishna Basin and Western Ghats of the Deccan Traps, India: Rates of basalt weathering and their controls. *Geochim. Et Cosmochim. Acta* **2005**, *69*, 2067–2084. [[CrossRef](#)]
49. Huh, Y.; Tsoi, M.; Zaitsev, A.; Edmond, J. The fluvial geochemistry of the rivers of Eastern Siberia: I. Tributaries of the Lena River draining the sedimentary platform of the Siberian Craton. *Geochim. Et Cosmochim. Acta* **1998**, *62*, 1657–1676. [[CrossRef](#)]
50. Chetelat, B.; Liu, C.-Q.; Zhao, Z.; Wang, Q.; Li, S.; Li, J.; Wang, B. Geochemistry of the dissolved load of the Changjiang Basin rivers: Anthropogenic impacts and chemical weathering. *Geochim. Et Cosmochim. Acta* **2008**, *72*, 4254–4277. [[CrossRef](#)]
51. Ding, T.; Gao, J.; Tian, S.; Shi, G.; Chen, F.; Wang, C.; Luo, X.; Han, D. Chemical and isotopic characteristics of the water and suspended particulate materials in the Yangtze River and their geological and environmental implications. *Acta Geol. Sin. Engl. Ed.* **2014**, *88*, 276–360. [[CrossRef](#)]
52. Fuoco, I.; De Rosa, R.; Barca, D.; Figoli, A.; Gabriele, B.; Apollaro, C. Arsenic polluted waters: Application of geochemical modelling as a tool to understand the release and fate of the pollutant in crystalline aquifers. *J. Environ. Manag.* **2022**, *301*, 113796. [[CrossRef](#)] [[PubMed](#)]
53. Zongxing, L.; Qi, F.; Wei, L.; Tingting, W.; Aifang, C.; Yan, G.; Xiaoyan, G.; Yanhui, P.; Jianguo, L.; Rui, G. Study on the contribution of cryosphere to runoff in the cold alpine basin: A case study of Hulugou River Basin in the Qilian Mountains. *Glob. Planet. Chang.* **2014**, *122*, 345–361. [[CrossRef](#)]
54. Yidana, S.M.; Ophori, D.; Banoeng-Yakubo, B. A multivariate statistical analysis of surface water chemistry data—The Ankobra Basin, Ghana. *J. Environ. Manag.* **2008**, *86*, 80–87. [[CrossRef](#)] [[PubMed](#)]
55. Ustaoglu, F.; Tepe, Y.; Tas, B. Assessment of stream quality and health risk in a subtropical Turkey river system: A combined approach using statistical analysis and water quality index. *Ecol. Indic.* **2020**, *113*, 105815. [[CrossRef](#)]
56. Burke, A.; Present, T.M.; Paris, G.; Rae, E.C.M.; Sandilands, B.H.; Gaillardet, J.; Peucker-Ehrenbrink, B.; Fischer, W.W.; McClelland, J.W.; Spencer, R.G.M.; et al. Sulfur isotopes in rivers: Insights into global weathering budgets, pyrite oxidation, and the modern sulfur cycle. *Earth Planet. Sci. Lett.* **2018**, *496*, 168–177. [[CrossRef](#)]
57. Zeng, J.; Han, G. Rainwater Chemistry Reveals Air Pollution in a Karst Forest: Temporal Variations, Source Apportionment, and Implications for the Forest. *Atmosphere* **2020**, *11*, 1315. [[CrossRef](#)]
58. Liu, J.; Wang, F.; Cai, W.; Wang, Z.; Li, C. Numerical investigation on the effects of geological parameters and layered subsurface on the thermal performance of medium-deep borehole heat exchanger. *Renew. Energy* **2020**, *149*, 384–399. [[CrossRef](#)]
59. Guo, F.; Jiang, G.; Yuan, D.; Polk, J.S. Evolution of major environmental geological problems in karst areas of Southwestern China. *Environ. Earth Sci.* **2013**, *69*, 2427–2435. [[CrossRef](#)]
60. Liu, Q.; Gu, Z.; Lu, Y.; Xiao, S.; Li, G. Weathering processes of the dolomite in Shibing (Guizhou) and formation of collapse and stone peaks. *Environ. Earth Sci.* **2015**, *74*, 1823–1831. [[CrossRef](#)]
61. Zeng, J.; Han, G.; Zhang, S.; Xiao, X.; Li, Y.; Gao, X.; Wang, D.; Qu, R. Rainwater chemical evolution driven by extreme rainfall in megacity: Implication for the urban air pollution source identification. *J. Clean. Prod.* **2022**, *372*, 133732. [[CrossRef](#)]
62. Zeng, J.; Han, G.; Zhang, S.; Qu, R. Nitrate dynamics and source identification of rainwater in Beijing during rainy season: Insight from dual isotopes and Bayesian model. *Sci. Total Environ.* **2023**, *856*, 159234. [[CrossRef](#)] [[PubMed](#)]
63. Grabb, K.C.; Ding, S.; Ning, X.; Liu, S.M.; Qian, B. Characterizing the impact of Three Gorges Dam on the Changjiang (Yangtze River): A story of nitrogen biogeochemical cycling through the lens of nitrogen stable isotopes. *Environ. Res.* **2021**, *195*, 110759. [[CrossRef](#)] [[PubMed](#)]
64. Xu, S.; Li, S.; Su, J.; Yue, F.; Zhong, J.; Chen, S. Oxidation of pyrite and reducing nitrogen fertilizer enhanced the carbon cycle by driving terrestrial chemical weathering. *Sci. Total Environ.* **2021**, *768*, 144343. [[CrossRef](#)] [[PubMed](#)]
65. Wang, B.; Lee, X.-Q.; Yuan, H.-L.; Zhou, H.; Cheng, H.-G.; Cheng, J.-Z.; Zhou, Z.-H.; Xing, Y.; Fang, B.; Zhang, L.-K.; et al. Distinct patterns of chemical weathering in the drainage basins of the Huanghe and Xijiang River, China: Evidence from chemical and Sr-isotopic compositions. *J. Asian Earth Sci.* **2012**, *59*, 219–230. [[CrossRef](#)]

66. Hui, T.; Jizhong, D.; Shimin, M.; Zhuang, K.; Yan, G. Application of water quality index and multivariate statistical analysis in the hydrogeochemical assessment of shallow groundwater in Hailun, northeast China. *Hum. Ecol. Risk Assess. Int. J.* **2021**, *27*, 651–667. [[CrossRef](#)]
67. Gibbs, R.J. Mechanisms controlling world water chemistry. *Science* **1970**, *170*, 1088–1090. [[CrossRef](#)] [[PubMed](#)]
68. Yang, R.; Sun, H.; Chen, B.; Yang, M.; Zeng, Q.; Zeng, C.; Huang, J.; Luo, H.; Lin, D. Temporal variations in riverine hydrochemistry and estimation of the carbon sink produced by coupled carbonate weathering with aquatic photosynthesis on land: An example from the Xijiang River, a large subtropical karst-dominated river in China. *Environ. Sci. Pollut. Res.* **2020**, *27*, 13142–13154. [[CrossRef](#)]
69. Han, Q.; Wang, B.; Liu, C.-Q.; Wang, F.; Peng, X.; Liu, X.-L. Carbon biogeochemical cycle is enhanced by damming in a karst river. *Sci. Total Environ.* **2018**, *616–617*, 1181–1189. [[CrossRef](#)]
70. Lü, J.; An, Y.; Wu, Q.; Zhou, S.; Wu, Y. Chemical characteristics and CO₂ consumption of the Qingshuijiang River Basin, Guizhou Province, Southwestern China. *Geochem. J.* **2018**, *52*, 441–456. [[CrossRef](#)]
71. Shen, B.; Wu, J.; Zhan, S.; Jin, M.; Saparov, A.S.; Abuduwaili, J. Spatial variations and controls on the hydrochemistry of surface waters across the Ili-Balkhash Basin, arid Central Asia. *J. Hydrol.* **2021**, *600*, 126565. [[CrossRef](#)]
72. Devic, G.; Djordjevic, D.; Sakan, S. Natural and anthropogenic factors affecting the groundwater quality in Serbia. *Sci. Total Environ.* **2014**, *468–469*, 933–942. [[CrossRef](#)] [[PubMed](#)]
73. Liu, J.; Peng, Y.; Li, C.; Gao, Z.; Chen, S. An investigation into the hydrochemistry, quality and risk to human health of groundwater in the central region of Shandong Province, North China. *J. Clean. Prod.* **2021**, *282*, 125416. [[CrossRef](#)]
74. Li, P.; Song, X.; Wang, J.; Zhou, X.; Li, J.; Lin, F.; Hu, Z.; Zhang, X.; Cui, H.; Wang, W.; et al. Reduced sensitivity to neutral feedback versus negative feedback in subjects with mild depression: Evidence from event-related potentials study. *Brain Cogn.* **2015**, *100*, 15–20. [[CrossRef](#)] [[PubMed](#)]
75. Liu, J.; Gao, Z.; Zhang, Y.; Sun, Z.; Sun, T.; Fan, H.; Wu, B.; Li, M.; Qian, L. Hydrochemical evaluation of groundwater quality and human health risk assessment of nitrate in the largest peninsula of China based on high-density sampling: A case study of Weifang. *J. Clean. Prod.* **2021**, *322*, 129164. [[CrossRef](#)]
76. Dun, Y.; Ling, J.; Wang, R.; Wei, J.; Zhou, Q.; Cao, Y.; Zhang, Y.; Xuan, Y. Hydrochemical Evolution and Nitrogen Behaviors in Coastal Groundwater Suffered From Seawater Intrusion and Anthropogenic Inputs. *Front. Mar. Sci.* **2022**, *9*, 945330. [[CrossRef](#)]
77. Xiao, J.; Jin, Z.D.; Wang, J.; Zhang, F. Hydrochemical characteristics, controlling factors and solute sources of groundwater within the Tarim River Basin in the extreme arid region, NW Tibetan Plateau. *Quat. Int.* **2015**, *380–381*, 237–246. [[CrossRef](#)]
78. Widory, D.; Petelet-Giraud, E.; Négrel, P.; Ladouche, B. Tracking the Sources of Nitrate in Groundwater Using Coupled Nitrogen and Boron Isotopes: A Synthesis. *Environ. Sci. Technol.* **2005**, *39*, 539–548. [[CrossRef](#)]
79. Fan, B.-L.; Zhao, Z.-Q.; Tao, F.-X.; Liu, B.-J.; Tao, Z.-H.; Gao, S.; Zhang, L.-H. Characteristics of carbonate, evaporite and silicate weathering in Huanghe River basin: A comparison among the upstream, midstream and downstream. *J. Asian Earth Sci.* **2014**, *96*, 17–26. [[CrossRef](#)]
80. Nijesh, P.; Akpataku, K.V.; Patel, A.; Rai, P.; Rai, S.P. Spatial variability of hydrochemical characteristics and appraisal of water quality in stressed phreatic aquifer of Upper Ganga Plain, Uttar Pradesh, India. *Environ. Earth Sci.* **2021**, *80*, 185. [[CrossRef](#)]
81. Liu, J.; Han, G. Controlling factors of riverine CO₂ partial pressure and CO₂ outgassing in a large karst river under base flow condition. *J. Hydrol.* **2021**, *593*, 125638. [[CrossRef](#)]
82. Zhang, Q.; Xu, P.; Qian, H.; Yang, F. Hydrogeochemistry and fluoride contamination in Jiaokou Irrigation District, Central China: Assessment based on multivariate statistical approach and human health risk. *Sci. Total Environ.* **2020**, *741*, 140460. [[CrossRef](#)] [[PubMed](#)]
83. Lundberg, J.O.; Weitzberg, E.; Cole, J.A.; Benjamin, N. Nitrate, bacteria and human health. *Nat. Rev. Microbiol.* **2004**, *2*, 593–602. [[CrossRef](#)] [[PubMed](#)]

Disclaimer/Publisher’s Note: The statements, opinions and data contained in all publications are solely those of the individual author(s) and contributor(s) and not of MDPI and/or the editor(s). MDPI and/or the editor(s) disclaim responsibility for any injury to people or property resulting from any ideas, methods, instructions or products referred to in the content.